



## Molecular Crystals and Liquid Crystals

Publication details, including instructions for authors and subscription information:

<http://www.tandfonline.com/loi/gmcl20>

### Design of a Highly Efficient Lightguide Plate Using an Anisotropic Layer with Polarization-Separating Microstructures

Seongmo Hwang<sup>a b</sup>, Youngchan Kim<sup>b</sup>, Yeun-Tae Kim<sup>a</sup>, Seungho Nam<sup>b</sup> & Sin-Doo Lee<sup>a</sup>

<sup>a</sup> School of Electrical Engineering, Seoul National University, Kwanak, Seoul, Korea

<sup>b</sup> Display Device and Processing Lab., Samsung Advanced Institute of Technology, Suwon, Korea

Version of record first published: 18 Mar 2009

To cite this article: Seongmo Hwang, Youngchan Kim, Yeun-Tae Kim, Seungho Nam & Sin-Doo Lee (2009): Design of a Highly Efficient Lightguide Plate Using an Anisotropic Layer with Polarization-Separating Microstructures, *Molecular Crystals and Liquid Crystals*, 499:1, 128/[450]-137/[459]

To link to this article: <http://dx.doi.org/10.1080/15421400802620055>

PLEASE SCROLL DOWN FOR ARTICLE

Full terms and conditions of use: <http://www.tandfonline.com/page/terms-and-conditions>

This article may be used for research, teaching, and private study purposes. Any substantial or systematic reproduction, redistribution, reselling, loan,

sub-licensing, systematic supply, or distribution in any form to anyone is expressly forbidden.

The publisher does not give any warranty express or implied or make any representation that the contents will be complete or accurate or up to date. The accuracy of any instructions, formulae, and drug doses should be independently verified with primary sources. The publisher shall not be liable for any loss, actions, claims, proceedings, demand, or costs or damages whatsoever or howsoever caused arising directly or indirectly in connection with or arising out of the use of this material.

## Design of a Highly Efficient Lightguide Plate Using an Anisotropic Layer with Polarization-Separating Microstructures

Seongmo Hwang<sup>1,2</sup>, Youngchan Kim<sup>2</sup>, Yeun-Tae Kim<sup>1</sup>,  
Seungho Nam<sup>2</sup>, and Sin-Doo Lee<sup>1</sup>

<sup>1</sup>School of Electrical Engineering, Seoul National University, Kwanak, Seoul, Korea

<sup>2</sup>Display Device and Processing Lab., Samsung Advanced Institute of Technology, Suwon, Korea

*We developed a highly efficient lightguide plate (LGP) using an anisotropic layer (AL) with polarization-separating microstructures. The microstructures were fabricated on a uniaxially stretched polymeric AL through a hot embossing process. Our LGP with asymmetric saw-tooth bistructures produces highly efficient polarized light along the direction normal to the AL by reducing the stray light propagating at large inclination angles. The backlight unit (BLU) with a newly designed LGP has about 30% higher luminance and integrated intensity than the conventional BLU with a reflective polarizer.*

**Keywords:** anisotropic layer; hot embossing; lightguide plate; luminance; polarization-separating microstructures

## INTRODUCTION

Recently, liquid crystal displays (LCDs) have been widely used for desktop computer monitors and high-definition television sets beyond notebook computer applications. The high brightness and low power consumption in the LCD depend critically on the performances of a backlight unit (BLU) which illuminates the LCD panel. In a conventional BLU, more than 50% of the unpolarized light is absorbed in

This work was supported in part by Samsung Electronics, AMLCD and in part by Korea Research Foundation Grant No. KRF-2004-005-D00165.

Address correspondence to Prof. Sin-Doo Lee, School of Electrical Engineering, Seoul National University, Kwanak P.O. Box 34, Seoul 151-600, Republic of Korea. E-mail: sidlee@plaza.snu.ac.kr

the rear polarizer. This large optical loss results in poor overall light efficiency of about only 5% in the LCD panel. Thus, much effort has been made toward improving the gain factor of the light efficiency by manipulating the polarized light in the BLU.

One approach is to integrate both the recycling capability and the polarizing function into a lightguide plate (LGP) which produces a linearly polarized light and recycles the light polarized orthogonal to it. In earlier works, a polarized LGP was composed of a multilayer sub-wave length grating as a polarizing beam splitter (PBS) [1,2]. This type of a polarized LGP has several drawbacks such as complicated manufacturing processes and limited tolerances in the wavelength and the incident angle. As an alternative, a polarized light illuminating system, based on a selective total internal reflection (TIR) at an interface between an isotropic layer and an anisotropic layer, was proposed and its feasibility was demonstrated in a small sample [3–5]. This illuminating system involves a diamond-cutting process of an anisotropic material which is not practically applicable for large LGPs [3,4], or a lamination process of a liquid crystalline polymer which causes the reliability problem of de lamination [5].

In this paper, we developed a highly efficient LGP using an anisotropic layer (AL) with polarization-separating microstructures that were fabricated on a uniaxially stretched polymer layer through a hot embossing process. The asymmetric saw-tooth microstructures used in the LGP result in high light efficiency along the direction normal to the AL by reducing the stray light propagating at large inclination angles. Our BLU prototype adopting a newly designed LGP has about 30% higher luminance and integrated intensity than the conventional BLU with a reflective polarizer.

## Design of Polarization-Separating Microstructures

We first describe a polarized BLU consisting of a cold cathode fluorescent lamp (CCFL) as light source, a back reflector, and a flat LGP on which a microstructured AL is laminated using a photo-curable isotropic adhesive as shown in Figure 1(a). The microstructured AL is laminated on the LGP with its optic axis along the s-polarization direction. The s-polarized light is out-coupled whereas the p-polarized light, present in the LGP, is recycled. The extraordinary and two ordinary refractive indices are denoted by  $n_e$ ,  $n_{o1}$ , and  $n_{o2}$ , respectively. The unpolarized light from a light source is selectively polarized and out-coupled at the microstructured interface between an isotropic layer and an anisotropic layer. Numerical simulations of the optical performances such as the polarization separation, total extracted light

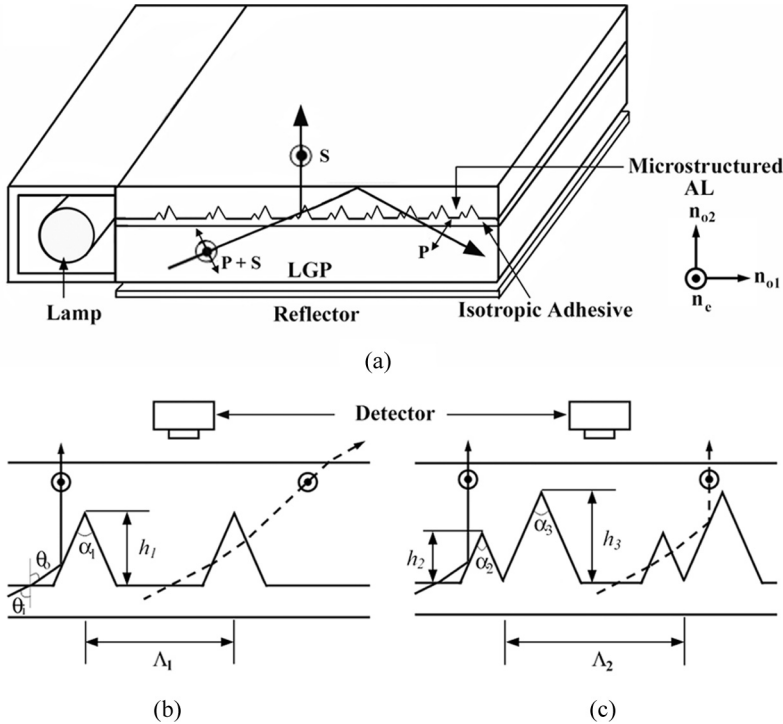


**FIGURE 1** The BLU adopting an LGP with a polarization-separating AL: (a) the schematic diagram of the edge-lit configuration, (b) the AL with a single prism array, and (c) the AL with an asymmetric bistructure array. The pitch, the height and the apex angle are defined as  $\Lambda_1$ , (or  $\Lambda_2$ ),  $h_1$  (or  $h_2$  and  $h_3$ ), and  $\alpha_1$  (or  $\alpha_2$  and  $\alpha_3$ ), respectively. The incident angle and the outgoing angle are represented by,  $\theta_1$  and  $\theta_0$ , respectively.

flux, and the angular distribution of luminous intensity were performed using a commercially available optical simulation and analysis program, Advanced System Analysis Program (ASAP, BRO Inc.), for the Monte Carlo ray tracing of the polarized light in a birefringent material. The extraordinary rays experience the TIR at the microstructured interface between the isotropic layer and the anisotropic layer. The angular distribution of the out-coupled rays was assumed to be collected by a detector with the diameter of 2 mm. Among the birefringent materials, a nearly uniaxial polyethylene terephthalate (PET) film was used as an AL due to the proper refractive index anisotropy. The extraordinary and ordinary refractive indices are  $n_e = 1.67$ ,  $n_{o1} = 1.56$  with a small biaxiality of 0.02 (giving

$n_{o2} = 1.54$ ). The adhesive layer has the refractive index ( $n_{adh} = 1.50$ ) similar to that of a polymethyl methacrylate (PMMA) LGP ( $n_{LGP} = 1.49$ ). The above refractive indices were determined using a prism coupler refractometer (2010 M, Metricon) at the wavelength of 532 nm.

For the AL with a conventional single prism array as shown in Figure 1(b), both the extracted s-polarized light flux and the inclination angle of the peak luminance increase with increasing the apex angle of the prism  $\alpha_1$ . According to Snell's equations for the incident angle of  $\theta_i$  and the outgoing angle of  $\theta_o$ , only the rays whose incident angle  $\theta_i$  meets the condition,  $\sin^{-1}(n_{adh}/n_e) \sin \theta_i = \alpha_1$ , can be out-coupled along the normal direction denoted by a solid line in Figure 1(b). It was suggested [3–5] that the prism with the apex angle  $\alpha_1$ , of around  $50^\circ$  produces the maximum luminance of the out-coupled light along the normal direction at the expense of a certain amount of the extracted light flux. Note that the stray light flux is still produced at large inclination angles due to the mismatch with the TIR condition at the prism interface. The light ray propagated through the prism and extracted from the LGP is represented by a dashed line in Figure 1(b). In such a case that the out-coupled light has the peak luminance at a large inclination angle, additional optical films are required for redirecting the light flux to the normal direction. However, the use of additional optical films causes the reduction of the light efficiency.

Let us consider another type of the AL with asymmetric saw-tooth bistructures as shown in Figure 1(c), and examine how the stray rays at large inclination angles become reduced or the luminance along the direction normal to the AL becomes increased. These asymmetric bistructures in Figure 1(c) are expected to redirect the stray rays propagating through the first prism, represented as a dashed line, along the normal direction by the adjacent second prism.

In terms of the pitch, the height(s), and the apex angle(s) for the prism structure(s), numerical simulations for the s-polarized light were carried out to calculate the distribution of the luminous intensity as a function of the inclination angle at the central wavelength of 550 nm. It is noted that variations of the height  $h_1$  have no significant effect on the angular distribution of the luminous intensity. A flat region of about  $20\ \mu\text{m}$  between the prisms was used for effectively out-coupling the extraordinary rays at the microstructured interface [5]. Thus, for the single prism array, the values for the geometrical parameters of  $\Lambda_1 = 35\ \mu\text{m}$ ,  $h_1 = 10\ \mu\text{m}$ , and  $\alpha_1 = 50^\circ$  were taken for the simulations. Figure 2(a) shows the luminous intensity as a function of the inclination angle. The luminous intensity along the normal was  $0.9\ \text{lm/sr}$  and the stray light at large inclination angles above

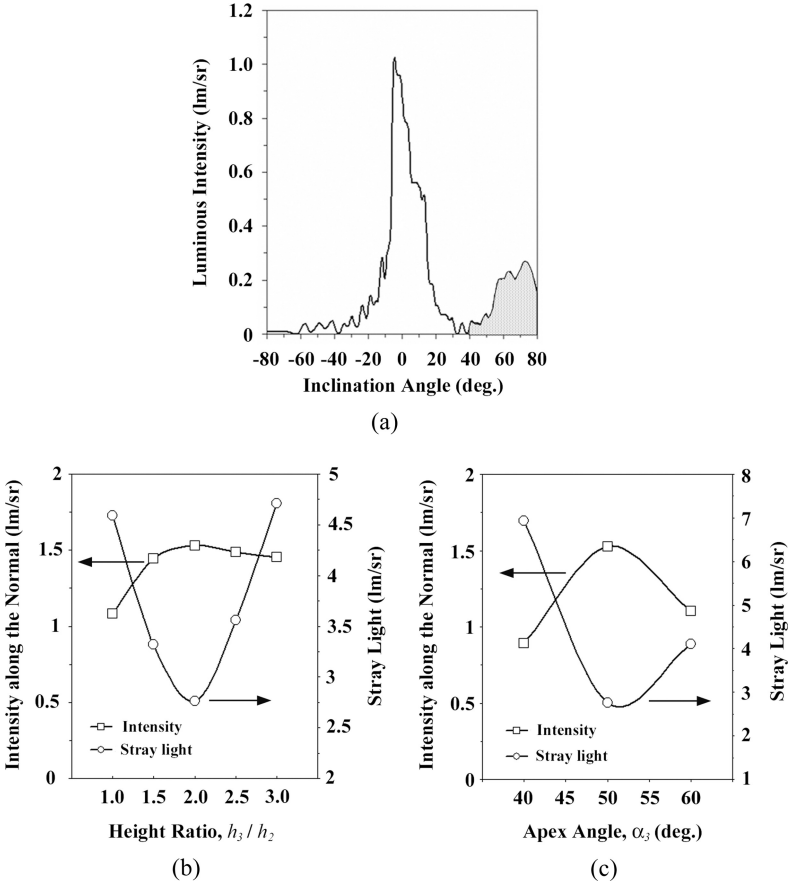


**FIGURE 2** The ray tracing simulation results for the luminous intensity along the normal and the amount of stray light at large inclination angles: (a) the luminous intensity of the LGP having the AL with single prisms, (b) the dependence of the height ratio  $h_2/h_3$ , and (c) the dependence of the apex angle  $\alpha_3$  for the LGP having the AL with asymmetric bistructures, respectively. The hatched area in (a) represents the total stray light above  $\theta=40^\circ$ .

$\theta=40^\circ$ , represented as hatched area in Figure 2(a), was 5.8lm/sr. As discussed above, it is evident that the significant amount of the stray light is produced at large inclination angles. For the purpose of reducing the stray light using the asymmetric bistructure array shown in Figure 1(c), we examine the effect of the height ratio  $h_3/h_2$  and the apex angle of  $\alpha_3$  on the luminous intensity along the normal direction and the amount of the stray light at large inclination angles

above  $\theta = 40^\circ$ . The pitch of  $\Lambda_2 = 50 \mu\text{m}$  was chosen in the same manner as the single prism array case. Figures 2(b) and (c) clearly show that the height ratio of  $h_3/h_2 = 2$  and the apex angle of  $\alpha_3 = 50^\circ$  are the optimal conditions for the maximum luminous intensity along the normal and the minimum stray light. In other words, for the asymmetric bistructure array, the optimal geometrical parameters are  $\Lambda_2 = 50 \mu\text{m}$ ,  $h_2 = 10 \mu\text{m}$ ,  $h_3 = 20 \mu\text{m}$ , and  $\alpha_2 = \alpha_3 = 50^\circ$ . The luminous intensity along the normal was calculated as 1.5 lm/sr and the stray light at large inclination angles above  $\theta = 40^\circ$  was 2.8 lm/sr. This tells us that compared to the single prism array, the luminous intensity increases and the stray light above  $\theta = 40^\circ$  decreases by more than 50% in the asymmetric bistructure array case.

### Fabrication of Microstructured Anisotropic Layer

Based on our simulation results shown in Figures 2(b) and (c), we fabricated a newly designed LGP with a polarization-separating AL made of a uniaxially stretched PET film of about  $100 \mu\text{m}$  thick. The asymmetric bistructures were produced on the PET substrate through a hot embossing process [6,7]. The PET was first heated above its glass transition temperature  $T_g$  (about  $80^\circ\text{C}$ ), and a periodic array of single prisms or asymmetric bistructures were produced on it by a stamp with designed patterns. The PET was then cooled below  $T_g$  before separating the stamp from it. It is important to maintain the pressure imposed on the PET to prevent any relaxation of the oriented molecules in the patterns till cooling the substrate down to room temperature. Details of the hot embossing process were shown in Figure 3(a) as a function of time. The hot embossing process was carried out at a temperature of  $200^\circ\text{C}$  under a nominal pressure of about  $290 \text{ kg/cm}^2$  for 5 min. The embossed microstructures on the PET were shown in Figures 3(b) and (c). From the cross-sectional view of the single prism in Figure 3(b) and that of the asymmetric bistructure in Figure 3(c), the microstructure patterns were found to be reasonably well replicated by the stamp. The measured geometrical parameters of the embossed microstructures were  $\Lambda_1 = 36 \mu\text{m}$ ,  $h_1 = 10 \mu\text{m}$  and  $\alpha_1 = 50^\circ$  for single prisms, and  $\Lambda_2 = 51 \mu\text{m}$ ,  $h_2 = 11 \mu\text{m}$ ,  $h_3 = 20 \mu\text{m}$  and  $\alpha_2 = \alpha_3 = 50^\circ$  for asymmetric bistructures. Note that these values are consistent with the optimal geometrical parameters determined from the ray tracing simulations. Each hot-embossed PET film was then laminated onto the PMMA LGP using an isotropic adhesive resin. The adhesive layer was subsequently cured by the exposure of ultra-violet light.

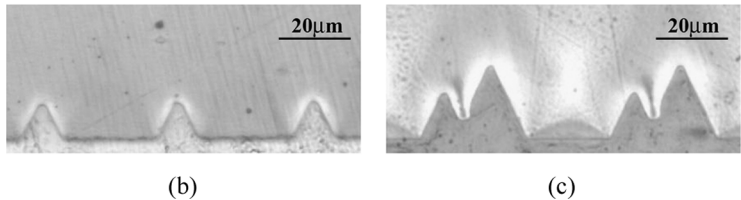
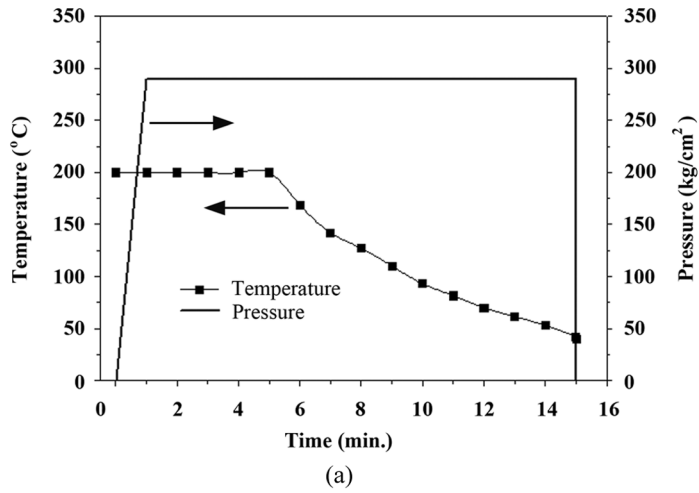


**FIGURE 3** A hot embossing process: (a) experimental results, (b) the cross-sectional view of the hot-embossed PET substrates with single prisms, and (c) the cross-sectional view of asymmetric bistructures, observed with an optical microscope.

## RESULTS AND DISCUSSION

We now measure the optical performances of a BLU adopting our LGP in the CCFL edge-lit configuration. The experimental geometry shown in Figure 4(a) was used in combination with a conoscope (EZContrast 160 R, Eldim). A white paper reflector was placed on the bottom of the LGP without using any optical film. A polarizer was inserted between the LGP and a detector with the diameter of 2 mm assembled into the conoscope. The transmission axis of the polarizer was either in parallel or in perpendicular to the optic axis of the AL. Along the normal direction, the measured luminance of the s-polarized light from the LGP with bistructures ( $3060 \text{ cd/m}^2$ ) was found to be nearly 50% higher than that of the LGP with single prisms ( $2016 \text{ cd/m}^2$ ). Our BLU produces significantly more s-polarized light (when the transmission axis of the polarizer coincides with the optic axis of the AL, see Fig. 1) than

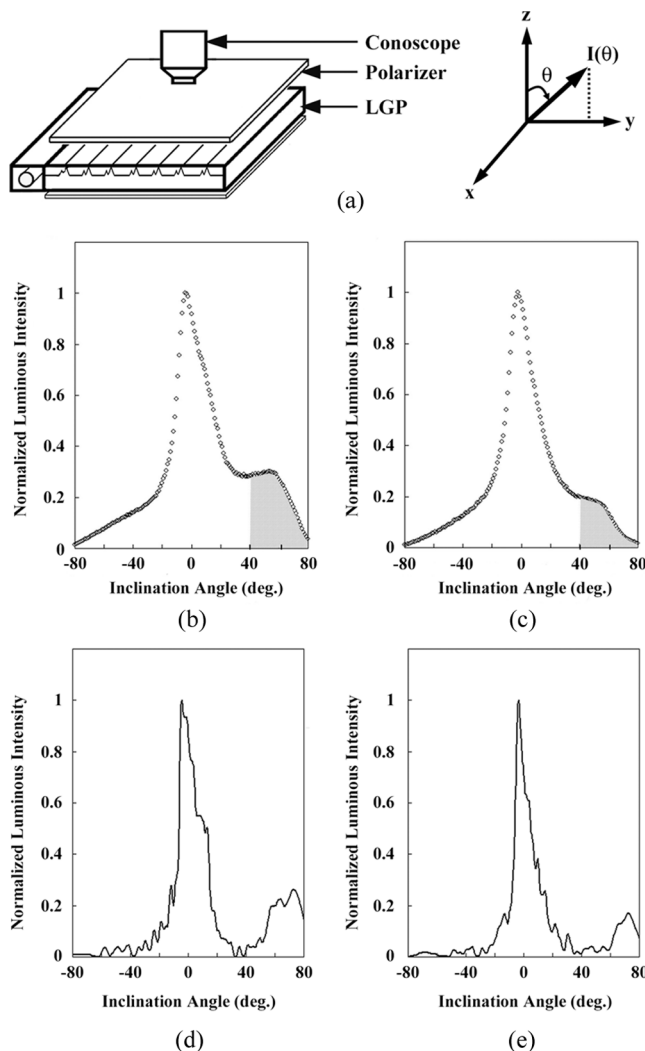


**FIGURE 4** The normalized luminous intensity for the s-polarized light as a function of the inclination angle for fixed azimuth angle of  $\varphi = 90^\circ$ : (a) the experimental setup, (b) and (d) are the measured and simulation results for the LGP having the AL with single prisms, and (c) and (e) are those for the LGP having the AL with asymmetric bistructures, respectively. Each hatched area in (b) and (c) represents the total stray light at large inclination angles above  $\theta = 40^\circ$ . The geometrical parameters are  $\Lambda_1 = 36 \mu\text{m}$ ,  $h_1 = 10 \mu\text{m}$ ,  $\alpha_1 = 50^\circ$  for single prisms and  $\Lambda_2 = 51 \mu\text{m}$ ,  $h_2 = 11 \mu\text{m}$ ,  $h_3 = 20 \mu\text{m}$ , and  $\alpha_2 = \alpha_2 = 50^\circ$  for asymmetric bistructures.

the p-polarized light along the direction normal to the AL. The ratio of the s-polarized light luminance to the p-polarized light luminance along the normal direction was about 9. Our BLU adopting the LGP with asymmetric bistructures showed at least 30% higher luminance and integrated intensity than a conventional BLU consisting of an LGP, a diffuser sheet, a prism sheet, and a reflective polarizer made up of a dual brightness enhancement film [8].

The luminous intensity,  $I(\theta)$ , was measured as a function of the inclination angle for fixed azimuth angle of  $\varphi = 90^\circ$  (along the  $y$ -direction). Figures 4(b) and (c) show the normalized luminous intensity for the AL with single prisms and that for the AL with asymmetric bistructures, respectively. Let us compare the experimental results with the simulation results in Figures 4(d) and (e). The qualitative features of each measured luminous intensity were well consistent with the simulations. The most important point is that at large inclination angles above  $\theta = 40^\circ$ , the stray light for the AL with single prisms was reduced by more than 50% in the AL with asymmetric saw-tooth bistructures due to the redirection of the stray rays, propagating through the first prism, to the normal direction of the AL by the adjacent second prism. This is clearly seen from the hatched regions in Figures 4(b) and (c). In an ideal case, the simulations show that the luminous intensity near the inclination angle of  $\theta = 40^\circ$  is negligible. However, the experimental results show a substantial amount of the intensity near  $\theta = 40^\circ$ . This is attributed partly to the possible index gradient produced in the PET during the hot embossing process across the microstructured interface between the isotropic layer and the anisotropic layer, which results in the brightness variations near the interfaces shown in Figures 3(b) and (c), and partly to the geometric shape which was not sharply defined. The roundness in prism tips causes the broadening of the distribution of the out-coupled rays.

## CONCLUSION

We developed a highly efficient BLU prototype adopting an LGP based on the AL with polarization-separating saw-tooth bistructures. By the reduction of the stray light flux at large inclination angles, the luminance of the s-polarized light along the direction normal to the AL was greatly increased. This leads directly to the enhancement of the contrast ratio of the LCD panel. Our BLU showed at least 30% higher luminance and integrated intensity than a conventional BLU with a reflective polarizer. As a consequence, our BLU needs less fabrication processes and is cost-effective because no additional optical element is required. Moreover, the LGP technology presented here is expected to

play a significant role in the production of large BLUs since the whole steps of uniaxial stretching, hot embossing, and lamination of the AL are potentially applicable for in-line roll-to-roll processes.

## REFERENCES

- [1] Chien, K.-W., & Shieh, H.-P. D. (2004). *Appl. Opt.*, *43*, 1830.
- [2] Yang, X., Yan, Y., & Jin, G. (2006). *Appl. Phys. Lett.*, *88*, 221109.
- [3] Chien, K.-W., Shieh, H.-P. D., & Cornelissen, H. (2004). *Appl. Opt.*, *43*, 4672.
- [4] Chien, K.-W., Shieh, H.-P. D., & Cornelissen, H. (2005). *Jpn. J. Appl. Phys.*, *44*, 1818.
- [5] Cornelissen, H. J., Huck, H. P. M., Broer, D. J., Picken, S. J., Bastiaansen, C. W. M., Erdhuisen, E., & Maaskant, N. (2004). *SID Int. Symp. Dig. Tech. Pap.*, *35*, 1178.
- [6] Shan, X. C., Maeda, R., & Murakoshi, Y. (2003). *Jpn. J. Appl. Phys.*, *42*, 3859.
- [7] Juang, Y.-J., Lee, L. J., & Koelling, K. W. (2002). *Polym. Eng. Sci.*, *42*, 539.
- [8] Weber, M. F., Stover, C. A., Gilbert, L. R., Nevitt, T. J., & Ouderkirk, A. J. (2000). *Science*, *287*, 2451.